Mapping the Risk of International Infectious Disease Spread (MRIIDS)

A project funded through USAID's "Combating Zika and Future Threats: A Grand Challenge for Development" program

Milestone 6: Increased complexity of the simple model to include data from Milestone 5.

Contents

1 Milestone Description

Increased complexity of the simple model to include data from Milestone 5. Automated testing and validating procedures implemented where possible. Explore procedures for multiple models comparison and accounting for uncertainty.

2 General Approach

In Milestone 4, we presented a simple transmission model that made use of historical case counts (data stream 1), information about the transmissibility of the pathogen (data stream 2) and geographical characterization (data stream 3) to predict future risk. In this approach, the geographical characterization was not fully integrated in the model: first transmissibility was estimated from case count data, then future incidence was predicted, and finally, the predicted incidence was distributed geographically according to the spatial distribution and population density of each geographical unit.

To achieve the goals outlined in Milestone 6, we built on the model presented in Milestone 4 (ML4) to integrate geographical information into our inference procedure. Having achieved this, other characteristics defined at the geographical scale of reference such as the health care capacity of a location, can be added to the model.

In essence, by integrating the spatial information into the inference and prediction phases, we have developed a complex model that has the potential to account for the multiple data streams initially described.

Therefore, our new complex model has the ability to:

- estimate model parameters: including parameters linked to geographical spread (or potentially health care capacity,
- predict the regional/international spread of Ebola, relying on those parameters' estimates.

We have also established the procedure for the validation process using historical data and are exploring various possibilities for multi-model comparison.

For the model validation, we rely on both Promed/HealthMap incidence data, which are at the national scale, and WHO reported data which are at the district level. The advantage of using the more spatially refined WHO data is that it allows increased statistical power to infer the spatial parameters of the model (i.e. more movements occur at finer spatial scale, therefore the 'signature' of movement in incidence data is more identifiable at finer scale). This exercise could be viewed as:

- demonstrating the flexible nature of our framework, i.e. the model is designed to be flexible in term of the choice of spatial scale, and
- a proof of concept to argue that reporting spatially refined incidence count can improve our ability to predict spatial spread.

3 Presentation of the model

The number of cases at a location j at time t is given by the equation

$$I_{j,t} \sim Pois\left(\sum_{i=1}^{n}\left(p_{i\to j}R_{t,i}\sum_{s=1}^{t}I_{i,t-s}w_s\right)\right),$$

where $R_{t,i}$ is the reproduction number at location i at time t and $p_{i\to j}$ is the probability of moving from location i to location j. The quantity $R_{t,i}$ is the reproduction number at time t at location i. $R_{t,i}$ is affected by a number of other factors e.g., the intrinsic transmissibility of a pathogen, the health care capacity at location i etc. Its dependence on these factors is formalized as

$$R_{t,i} := f(haq_i, R_0, t),$$

where haq_i is an index/score quantifying the health care capacity at location i, f denotes a function, R_0 is the basic reproduction number (data stream 2) and t is time..

The probability of moving between locations is derived from the relative flow of populations. This latter quantity is estimated using a population flow model such as a gravity model. Under a gravity model, the flow of individuals from area i to area j, $\phi_{i\to j}$, is proportional to the product of the populations of the two areas, N_i and N_j and inversely proportional to the distance between them $d_{i,j}$, all quantities are raised to some power.

$$\phi_{i\to j} := \frac{N_i^{\alpha}N_j^{\beta}}{d_{i,j}^{\gamma}}.$$

In practice, α and β are assumed to be 1. The exponent γ modulates the effects distance on the flow of populations. A large value of γ indicates that the distances traveled by populations tend to be short.

The relative risk of spread at a location j from a location i is thus the population flow into location j from location i.

$$r_{i\to j}^{spread} = \frac{\phi_{i\to j}}{\sum_x \phi_{i\to j}}.$$

The probability of movement from location i to location j is given by

$$p_{i\to j} = (1 - p_{stay}^{i})r_{i\to j}^{spread},$$

where p_{stay}^{i} is the probability of staying at location i. As the above equation indicates, by varying p_{stay}^{i}, we can capture the dynamics of population flow across spatial units. For instance, if p_{stay}^{i} is large, then the flow out of location i would be small. Thus, if this parameter is geographically heterogeneous, we obtain imbalanced flow of population (i.e. a source-sink dynamics).

3.1 Statistical inference of model parameters

The parameters of the full model as presented in Section 3 are:

- $R_{t,i}$, the reproduction at time t,
- p_{stay}, the probability of staying in location i, and
- γ, the exponent of the distance in the gravity model.

The parameters can be estimated using maximum likelihood estimation or estimating the posterior distribution of the parameters using MCMC. Let the observed incidence time series at locations 1 through n and time $1, 2 \dots t$ be

$$I = \begin{bmatrix} o_{1,1} & o_{1,2} & \dots & o_{1,n} \\ o_{2,1} & o_{2,2} & \dots & o_{2,n} \\ \dots & \dots & \dots & \dots \\ o_{t,1} & o_{t,2} & \dots & o_{t,n} \end{bmatrix}$$

where $o_{i,j}$ is the observed incidence at time i at location j. Then the likelihood of the model parameters given the observations is proportional to the probability of the data given model parameters. The probability of $o_{j,t}$ given the model parameters is:

$$P(o_{j,t} \mid p^i_{stay}, \gamma, R_{i,t}) = e^{-\lambda_{j,t}} \frac{o_{j,t}^{\lambda_{j,t}}}{\lambda_{j,t}!},$$

where $\lambda_{j,t}$ is given by

$$\lambda_{j,t} = \sum_{i=1}^{n} \left(p_{i \to j} R_{i,t} \sum_{s=1}^{t} I_{i,s} w_{t-s} \right).$$

Thus assuming that each observation is independent, the likelihood of the parameters is proportional to

$$\mathcal{L} = P(\{o_{j,t}\} \mid \{p^i_{stay}\}, \gamma, \{R_{i,t}\}) = \prod_{t=1}^{t} e^{-\lambda_{i,t}} \frac{o_{i,t}^{\lambda_{i,t}}}{\lambda_{i,t}!}.$$

In practice, we estimate $R_{t,i}$ as an average over the past 2 or 3 week with sliding time windows.

Given this likelihood, we can write the joint posterior distribution of the parameter given the observed data as:

$$P(\{p^i_{stay}\}, \gamma, \{R_{i,t}\} \mid \{o_{j,t}\}) \propto \mathcal{L} \times P(\{R_{i,0}\}) P(\{p^i_{stay}\}) P(\gamma).$$

Here, $P(\{R_{i,0}\})$ represents the prior distribution of the basic reproduction number. This prior distribution is influenced by data-stream 2 and the health capacity of the location i, as described above.

The other prior distributions, $P(\{p^i_{stay}\})$ and $P(\gamma)$, could in principle reflect the influence of additional data sources such as prior information derived from flight data.

3.2 Multi-model Comparison

Given the most general model formulation outlined above, multiple models could be formulated that can be viewed as simplification of the original model. For instance a model could assume $\{R_{i,t}\}$ to be constant across geographical units, or could assume that the parameter γ of the gravity model is 1.

Variants of the model would have distinct number of parameters, for instance assuming $\gamma = 1$ would reduce the number of parameters to be estimated by 1.

Relying on data-driven and evidence based approaches, we seek to formulate the simplest model that account for patterns observed in the data. In such a model, all layers of complexity must be justified, i.e. it is justified to estimate a parameter γ (and not assume unity) if and only if the fit of our model to the observed data is significantly improved (in a statistical sense).

Relying on our MCMC estimation of the joint posterior, we can evaluate the goodness of fit of any model by calculating the Deviance Information Criterion (DIC). DIC is a well established measure of goodness of fit, and is commonly used for model selection. It promotes models that can best reproduce observed patterns while penalizing for increased models complexity (i.e. increased number of parameters).

Using such a 'model selection' approach, each model is evaluated in turn, DICs are obtained and compared, and we can rigorously select the best model to produce the final predictions.

Alternatively, after evaluating each model, we can produce 'model averaged' predictions. Under this approach, the predictions of each model are weighted according to the statistical of the particular model. Such approach has the advantage of accounting for structural uncertainties, i.e. the very structure of the underlying model is treated as an unknown state.

The 'model averaged' predictions are finally obtained based on the 4 following steps:

- evaluate the goodness of fit (e.g. DIC) for each model,
- calculate the difference (Δ_k) between the DIC value of the best model and the DIC value for each of the other models,
- compute the relative weight for each model as $w_k = \frac{exp(\frac{1}{2}\Delta_k)}{\sum_{m=1}^{M} exp(\frac{1}{2}\Delta_m)}$, with M the total number of models evaluated,
- produce predictions by sequentially 1) randomly selecting a particular model according to its weight, 2) producing predictions based on the parameters' joint posterior distributions associated with this particular model.

We are currently in the process of implementing those approaches (simple model selection and multi-model averaging). Once implementation is finalized, we will validate and contrast both approaches, recognizing that while selecting a model is easier to implement, multi-model averaging should better account for both parameters and model uncertainty, i.e. parametric and structural uncertainties.

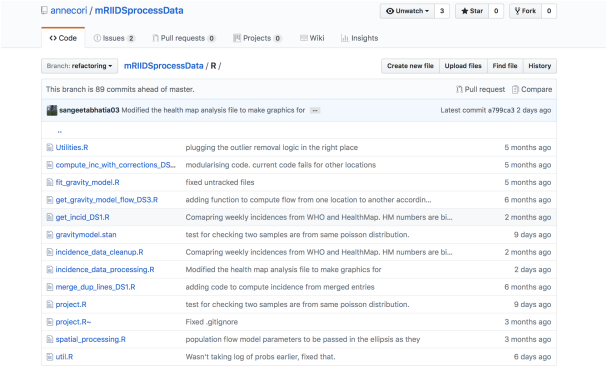

Figure 1: The software being developed for the project is available on GitHub.

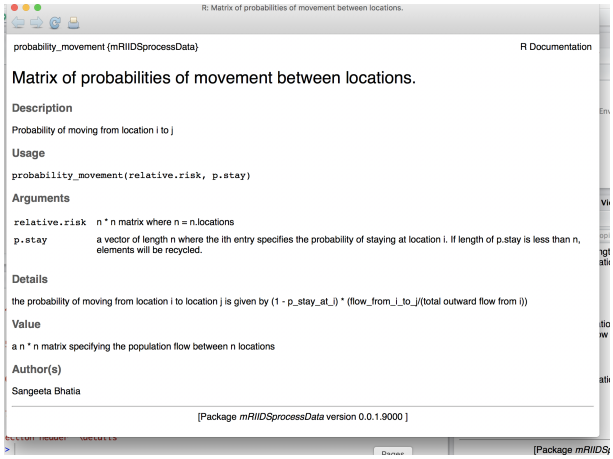

Figure 2: An example of the documentation for the R package mRIIDS

4 Implementation Details

4.1 Software Package mRIIDS

The general approach outlined above relies on several data streams, an inference framework, and a framework for projection. The code developed as part of the project is available as an open source R package that provide functions for pre-processing and collating the various data streams as well as plug the data into modules that will do the inference and the projection.

The software package will be published on the R packages repository (CRAN). At the moment, it is available on GitHub: github.com/annecori/mRIIDSprocessData (figure 1).

The package will include extensive documentation in the form of user-friendly help files and vignettes. An example of a help file can be seen in Figure 2.

4.2 Collating data for each data stream

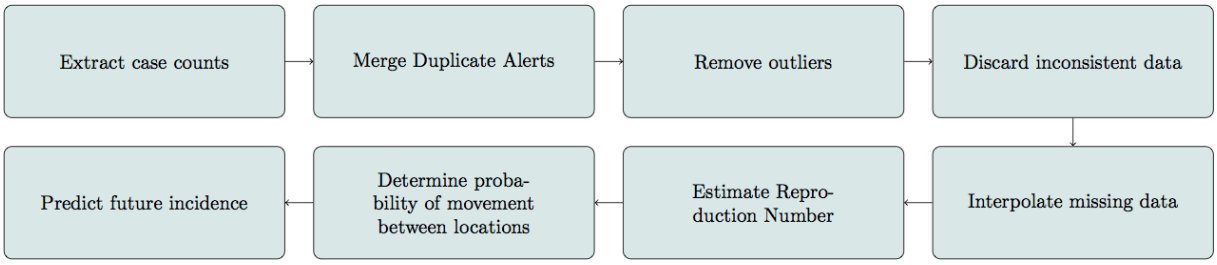

Figure 3: Workflow for the processing of the various data streams.

Figure 3 summarizes the steps involved in collating the different data streams and in going from raw data to predictions. In Milestone 6, a step was added to the data pre-processing workflow to remove outliers from data. The removal of outliers was done using Chebyshev Inequality with sample mean (see **?**). Figure 4 illustrates the results of each step in the pre-processing steps in the workflow.

4.3 Model training and validation using data from WHO

In the current iteration, the model was trained and validated the data on cases officially reported to the WHO during the 2013–2016 Ebola outbreak in Guinea, Liberia and Sierra Leone. This dataset was cleaned and published in [**?**] and it is this cleaned version of the data that were used in this work. This dataset consists of incidence reports at ADM2 level. Thus in using it, we were able to validate the model at a finer spatial resolution than available with HealthMap/ProMed data. We refer to this dataset as WHO data throughout the rest of this document.

4.4 Incidence trends from different data sources

We aggregated the WHO data to national level to compare the incidence trends derived from the three different data sources (WHO, HealthMap and ProMed). As can be seen in Figure 5, the incidence time series of the three data sources were well correlated.

During an emergency, such as the West Africa epidemics, spatially refined data (such as the WHO data are typically not available in real time due to reporting delay [REF cori, 2017 lesson learn]. A key advantage of relying on Promed/Health data in our project is the real time nature of the data. However this come at the cost of nationally aggregated data.

The results of the analysis above point toward a potential solution to obtain 'pseudo real-time' district level incidence data. One could relay on real-time national data (e.g. Promed/Healthmap) and disaggregate the time-series to obtain district level incidence using spatial information from a ' retrospective' time-series at finer scale (i.e. WHO data).

4.5 Inference of parameters

The parameters of the full model detailed in Section 3 are α, β, γ, p_{stay} and $R_{i,t}$. A simple estimation of $R_{i,t}$ can be obtained using incidence data and knowledge of the serial interval. Such statistical

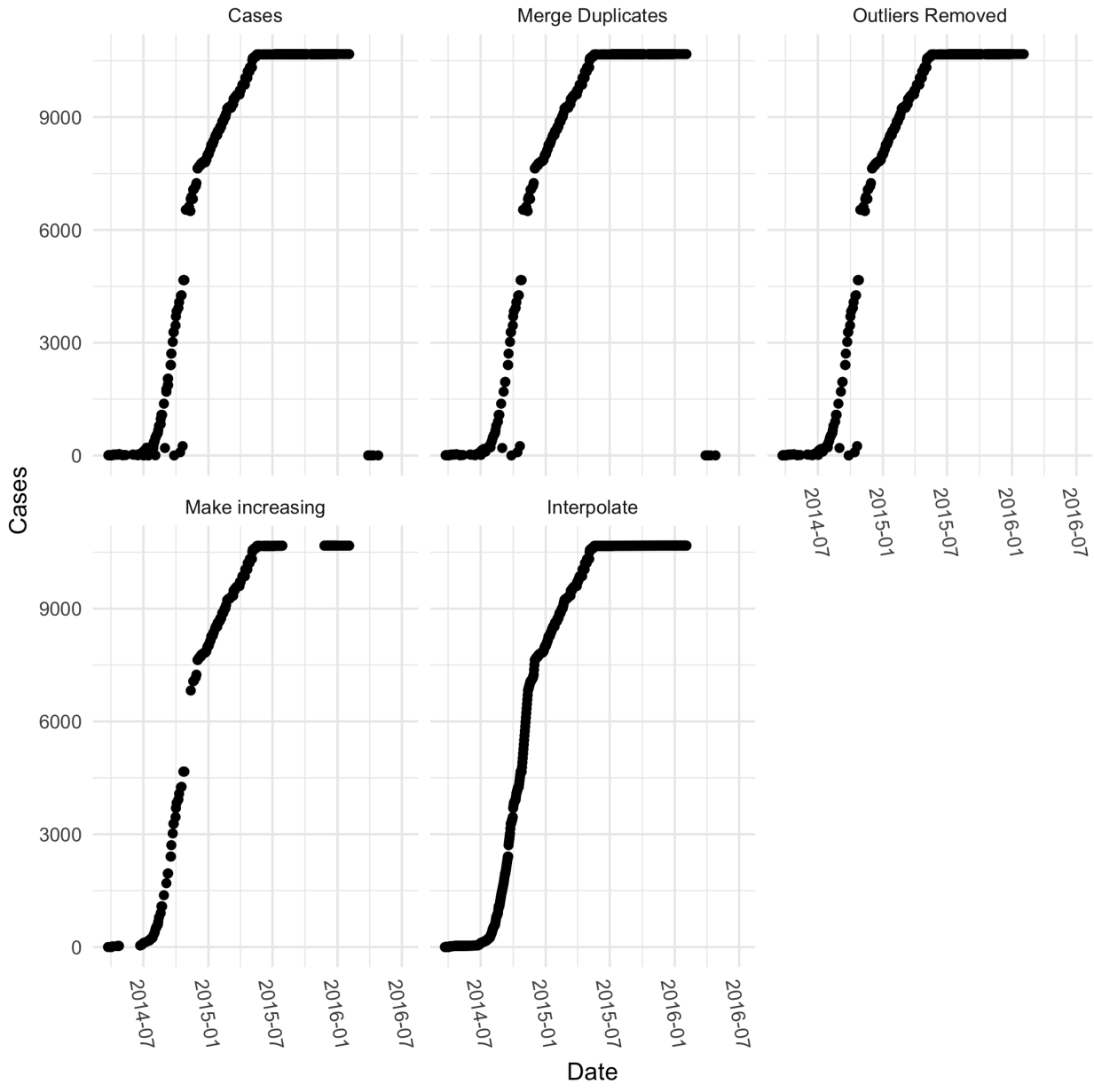

Figure 4: Illustration of the pre-processing steps on HealthMap incidence data for Liberia.

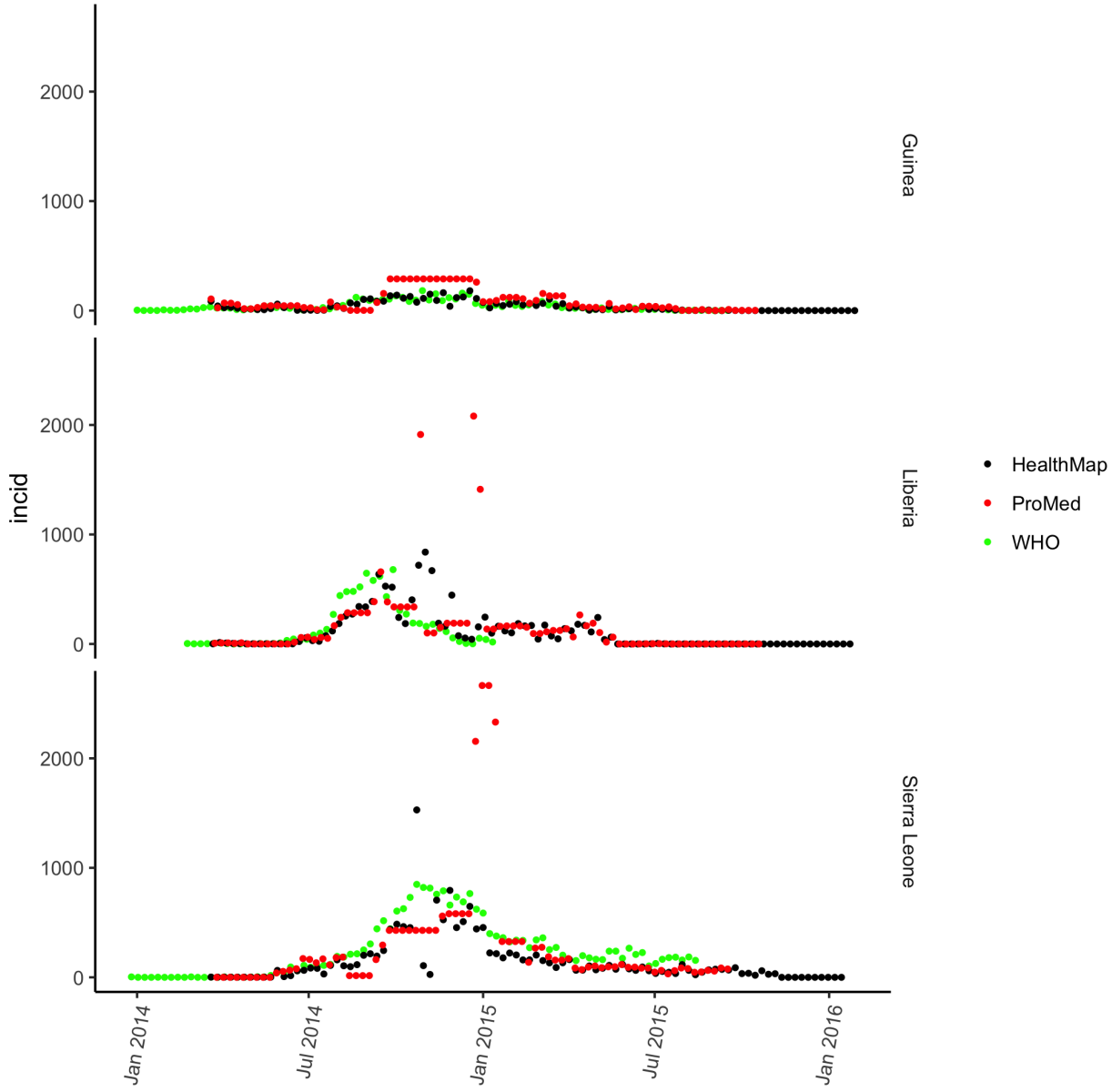

Figure 5: Comparison of incidence data from WHO, HealthMap and ProMed.

procedure has been implemented in the R package EpiEstim. Figure 6 shows the reproduction number estimated assuming constant transmissibility during period of 28 days. Sliding 28 days windows allow us to obtain daily estimate of the reproduction number (see [ref AJE cori] for details).

We estimated temporal pattern of the reproduction number for the 3 most affected country in West Africa using either data sources (Promed, Healthmap, and WHO). The high degree of correlation in the estimates of transmissibility from the three different data sources shows that the estimation procedure is robust to slight variations in reported incidence.

Then, the spatial spread must be assessed. In the interest of simplicity, we assume both α and β to be 1. The other two parameters are p_{stay} and γ. We explored the influence of these two parameters on the quality of fit of the predictions from the models at various points in the epidemic. To assess the goodness-of-fit, we used the normalised root mean squared error (rms), which is the sum of squares of the differences between observed and predicted values. That is,

$$rms := \sum_{i=1}^{n} (o_i - p_i)^2,$$

where o_i is ith observation, p_i is the corresponding value predicted by the model and n is the total number of observations.

4.6 Predicting Future Cases

As mentioned earlier, the WHO data consisted of incidence data at the district level. To validate the model, we carried out analysis at both the district level using WHO data and at country level using data from HealthMap.

4.6.1 Prediction at country level

Predictions over a 7 week period were carried out using the incidence data provided by HealthMap. The data pre-processing steps detailed in an earlier section were applied. The incidence obtained after these steps are shown in Figure 8.

The projection was done at two different time steps - at 200 days and 400 days from the start of the epidemic (October 2014 and April 2015 respectively) in order to capture an increasing as well as a decreasing phase in the outbreak. Figure 9 shows the predictions for October 2014. Figure 10 is the corresponding figure for projections in April 2015.

4.6.2 Prediction at district level

Predictions over a 7 week period were carried out at 2 different time points - at 300 and 500 days from the start of the epidemic (October 2014 and May 2015 respectively). [[In estimating the reproduction number, previous 7 weeks of incidence data were used, DONT understand, especially link with next sentence...]]. It is assumed that the transmissibility did not change for the previous 7 weeks (as in **?**). This analysis was carried at the sub-national levels for Sierra Leone, Liberia and Guinea as well as across the 55 districts in the three countries. Figure 11 illustrates the results for

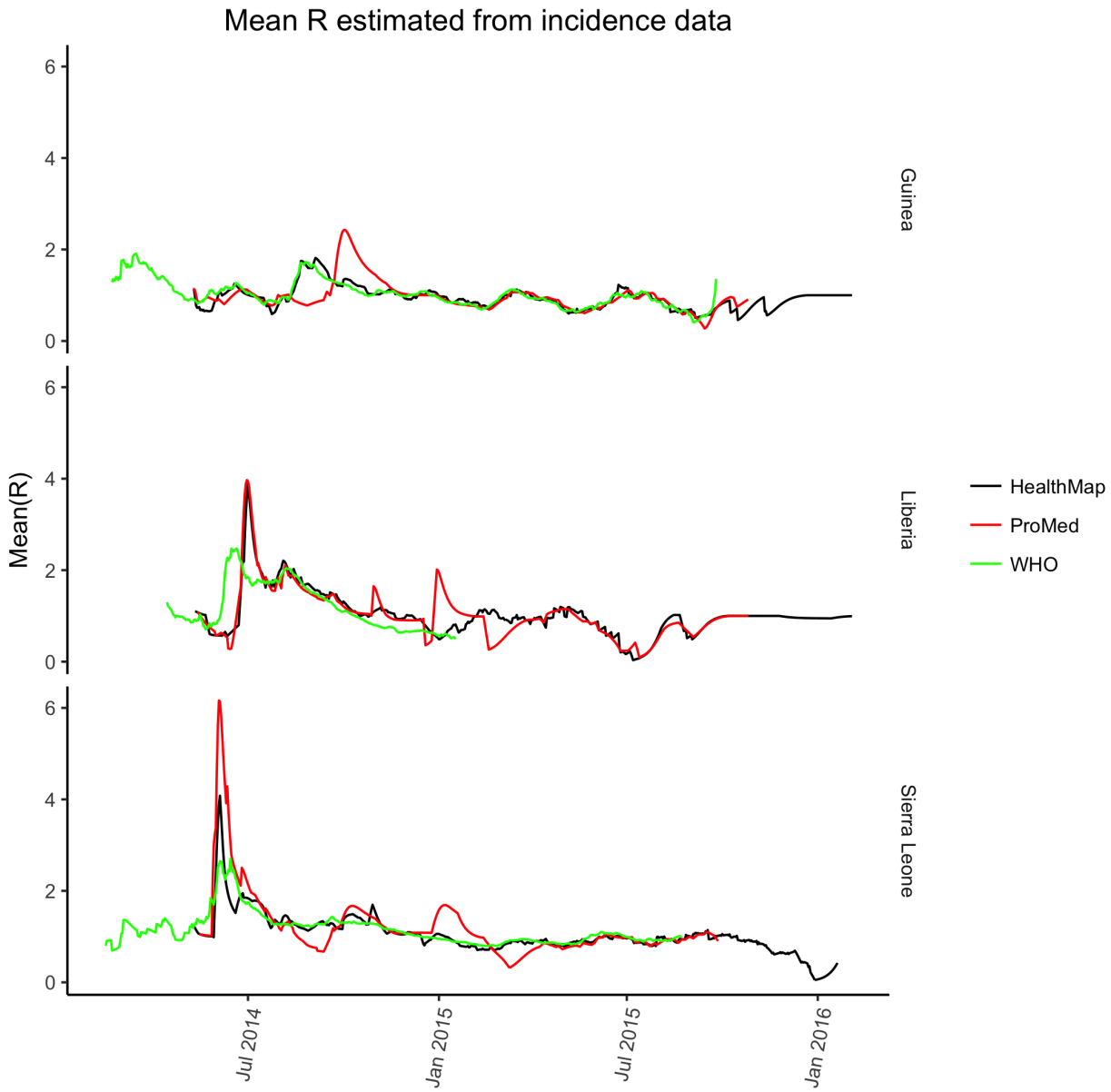

Figure 6: Comparison of the reproduction numbers estimated from the different sources of the incidence data.

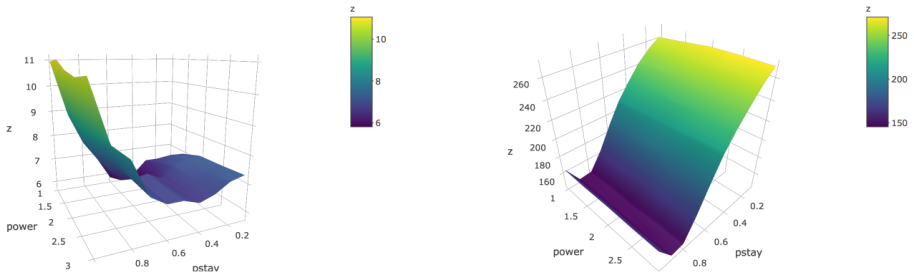

(a) Root mean square errors for prediction for 5 weeks at 100 days from the start of the epidemic.

(b) Root mean square errors for prediction for 5 weeks at 300 days from the start of the epidemic.

Figure 7: Normalised root mean squared error as a function of the model parameters. The fit is assessed for prediction of 5 weeks at 100 and 300 days from the start of the epidemic. The fit is better for smaller values of the root mean square error. In the early phase of the epidemic, a better fit is obtained at a smaller value of p_{stay} while at the 300 days mark, a much higher value of p_{stay} is needed to obtain a good fit.

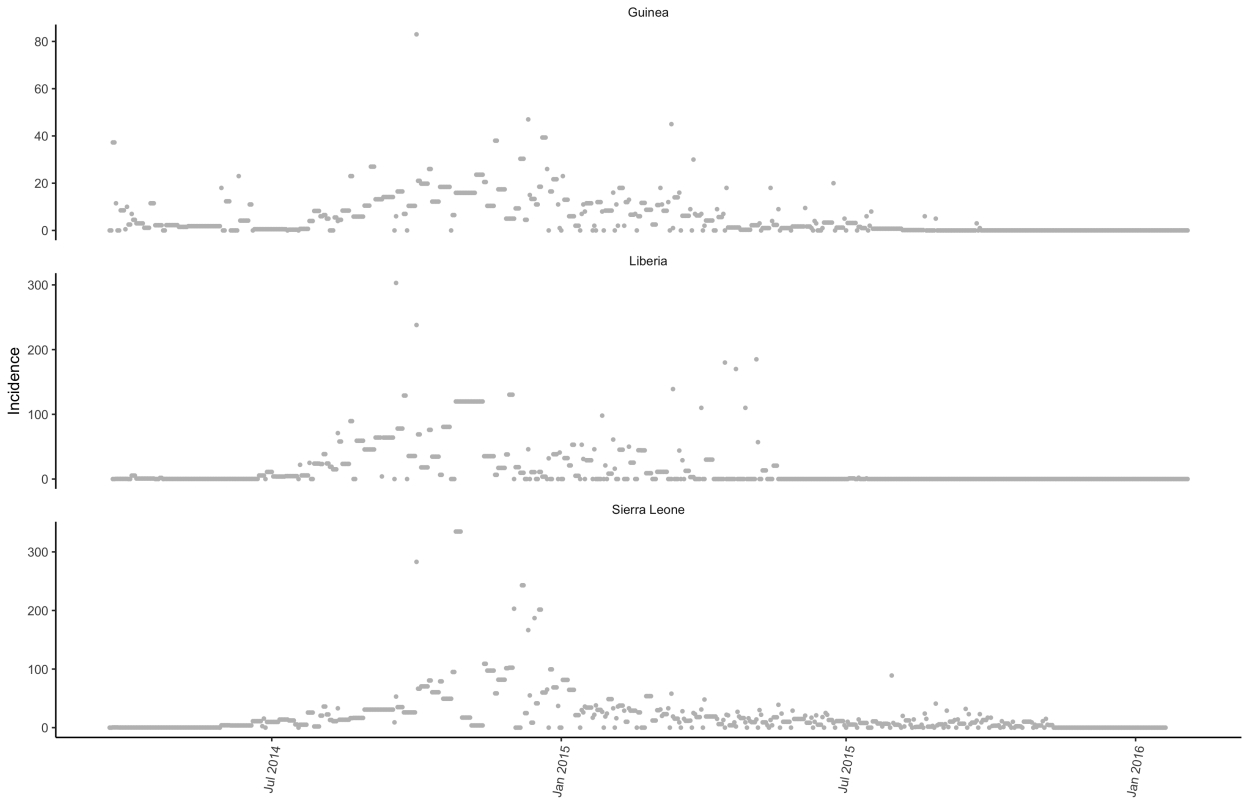

Figure 8: Incidence data from HealthMap after the pre-processing steps

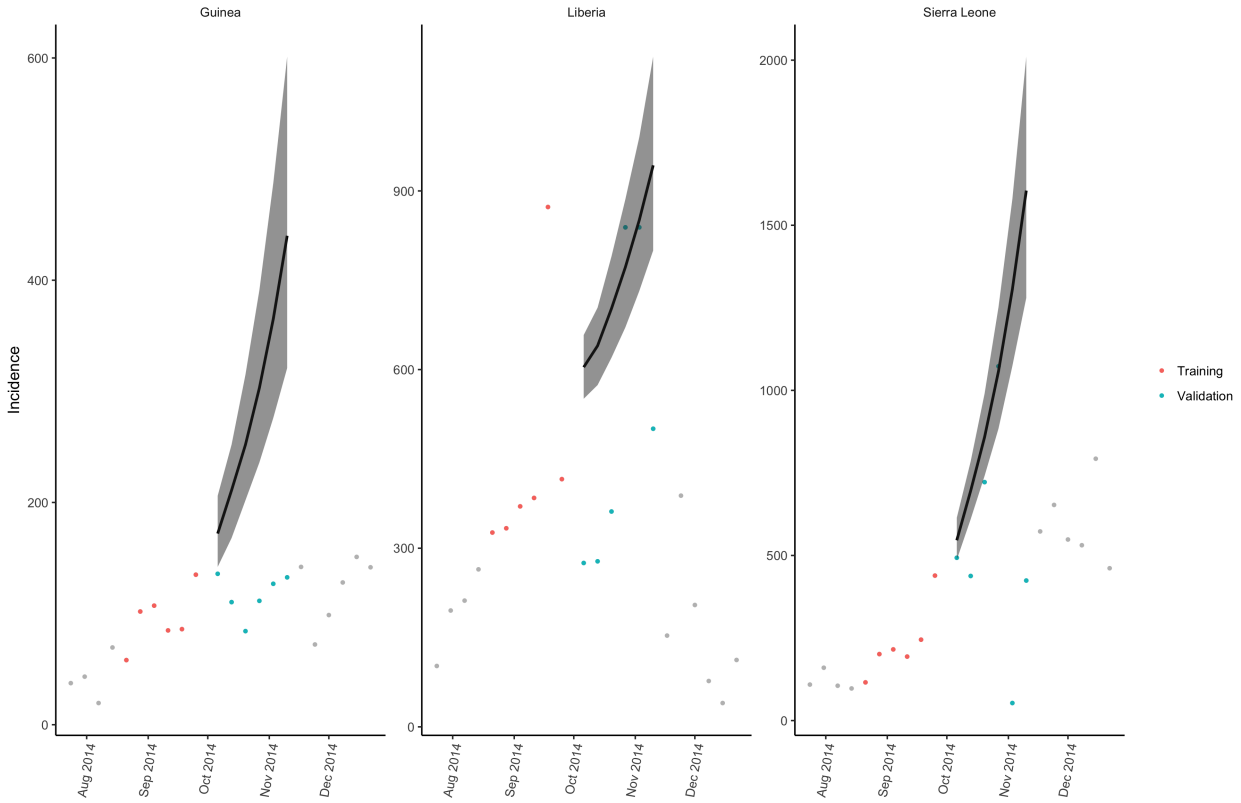

Figure 9: Predictions using HealthMap data in October 2014. The orange dots represent the data used to estimate the instantaneous reproduction number. The blue dates represent the observed incidence in the period over which prediction is being carried out. The solid black line traces the median projected incidence and the shaded area constitutes the 95% credible interval around the median incidence.

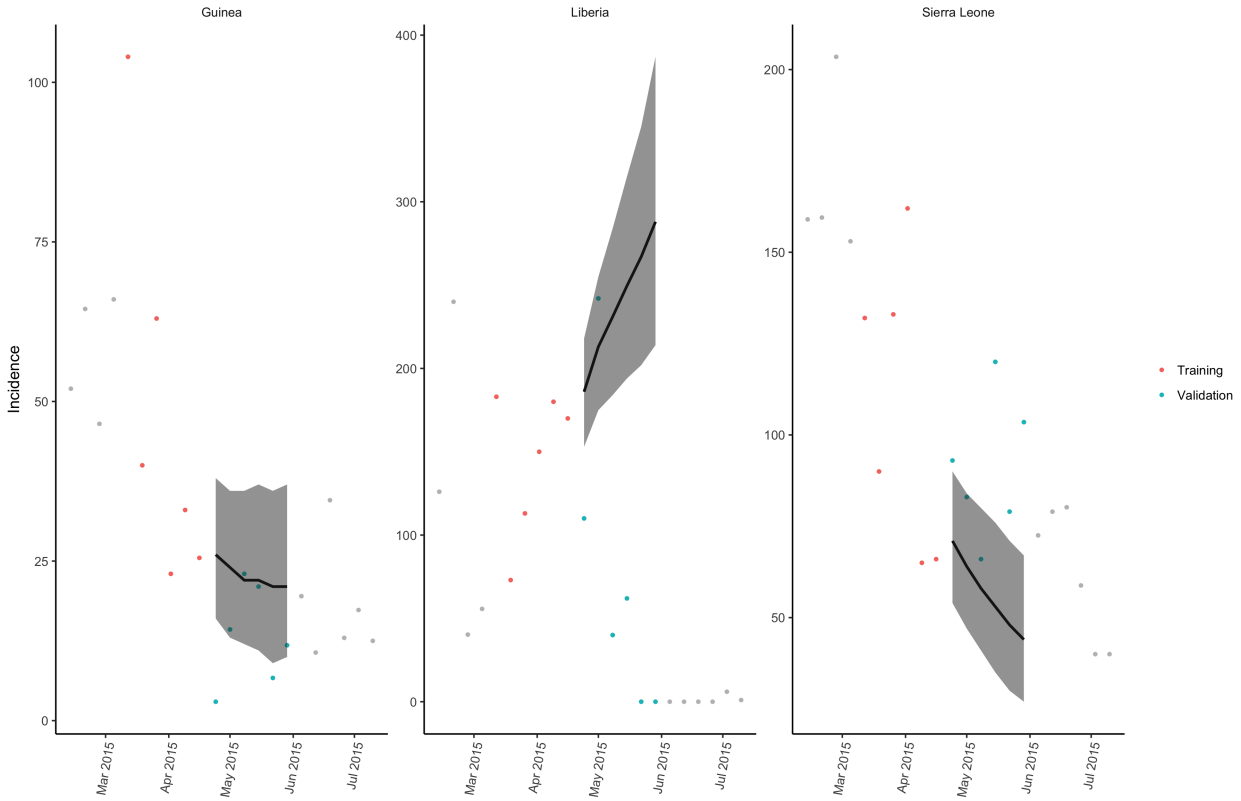

Figure 10: Predictions using HealthMap data in October 2014. The orange dots represent the data used to estimate the instantaneous reproduction number. The blue dates represent the observed incidence in the period over which prediction is being carried out. The solid black line traces the median projected incidence and the shaded area constitutes the 95% credible interval around the median incidence.

Sierra Leone. Figure 12 compared the observed and predicted spatial spread of the epidemic over a 7 week period beginning in May 2015. It can be seen that the model performs well at capturing the spatial dimension of the epidemic.

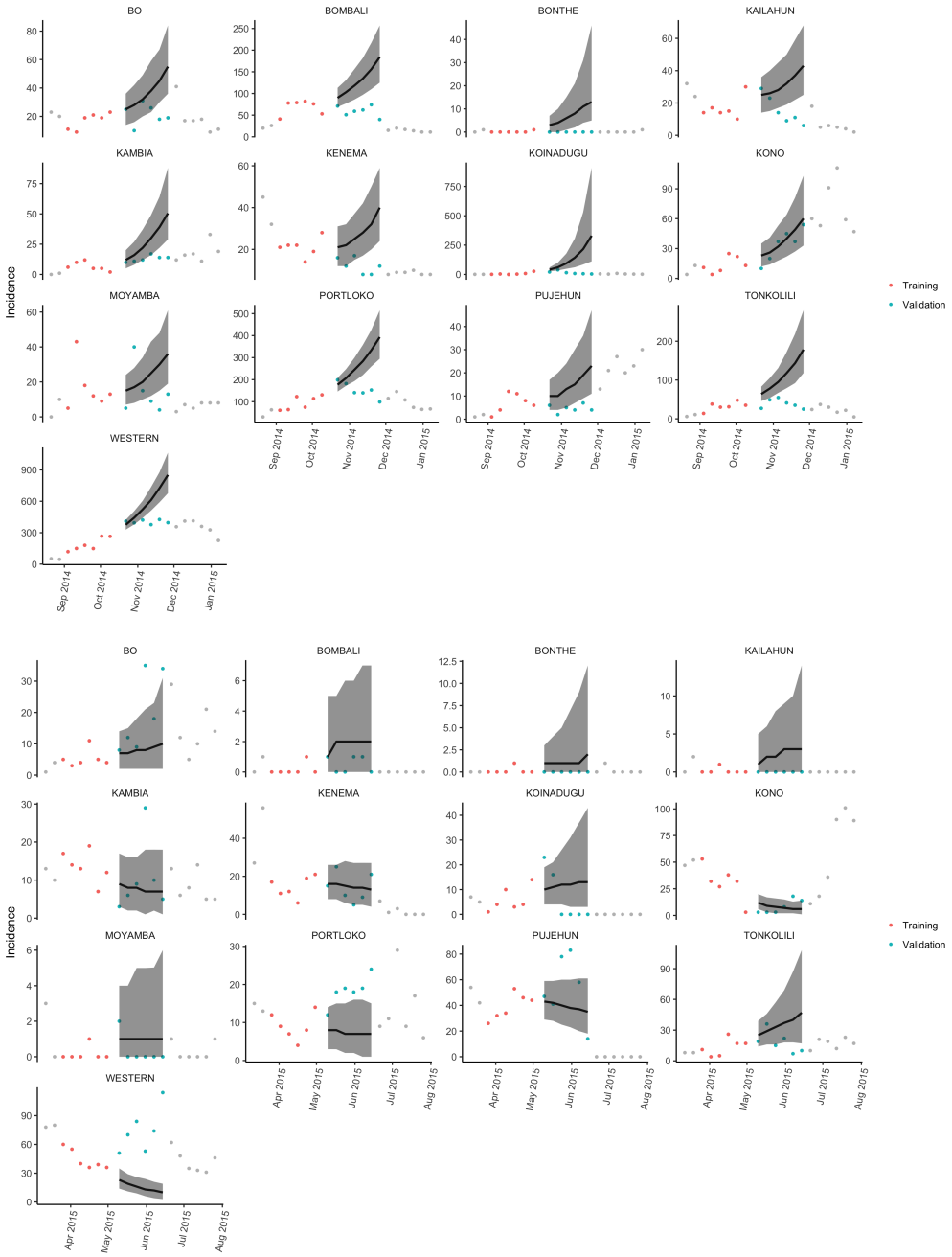

Figure 11: Spread of Ebola in the districts of Sierra Leone. Orange dots represent the data used to estimate the instantaneous reproduction number. Blue dots are the observed incidences in the period over which prediction is being carried out. Solid line represents the median predicted weekly incidence and the shaded area is the 95% credible interval. The top panel shows the predictions at 300 days from the start of the epidemic (October 2014) and the bottom panel is the prediction at 500 days (May 2015).

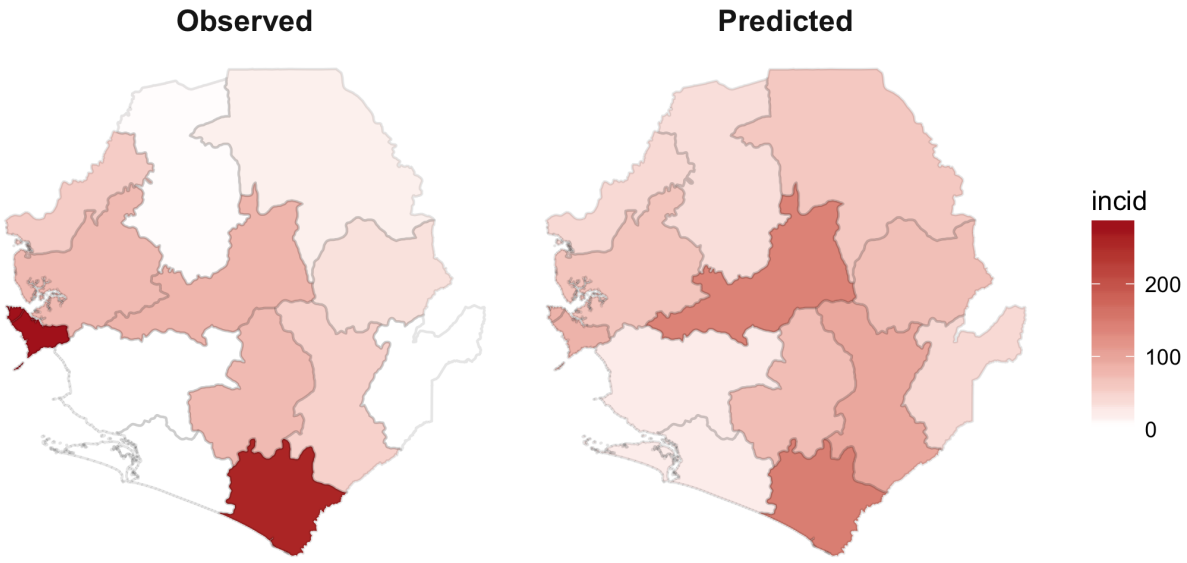

Figure 12: The map shows the observed (left) and predicted (right) spatial spread of Ebola in Sierra Leone over a 7 week period beginning in May 2015.

5 Conclusions and next steps

References

References